



## A New Vehicle Image Dynamic Tracking Approach

**Zhongwei LIANG, Bangyan YE**

School of Mechanical and Automobile Engineering, South China University of Technology  
Guangzhou, 510640, China  
Tel.: 13416240167, fax: 0862039366923  
E-mail: [lzwstalin@126.com](mailto:lzwstalin@126.com)

*Received: 20 November 2013 / Accepted: 27 December 2013 / Published: 28 February 2014*

---

**Abstract:** For the purpose of moving target's detecting, a new image tracking approach based on the changing factor of reference background learning and the direction predicting operator is presented. The high-speed moving vehicle is used as the detecting target for establishing a changing factor, on this basis the image sequence's reference background learning is conducted, then by cross-correlation matching and coordinate transforming the moving target-vehicle is coordinate-positioned and speed-determined, combining with the direction predicting operator the moving direction of the target vehicle is predicted, thus the vehicle image-tracking can be realized. Through tracking experiment and performance comparison it is proved that by this new approach an accurate and stable tracking results of moving vehicle can be gotten; a new idea can also be provided for the research of moving target's image-monitoring. *Copyright © 2014 IFSA Publishing, S. L.*

**Keywords:** Changing factor, Reference background, Direction predicting operator, Moving vehicle, Image tracking.

---

### 1. Introduction

Much attention has been attracted in image tracking of moving target. In 1997 the auto video-understanding monitoring has been studied by an a System for Video Surveillance and Monitoring project (VSAM) from Defense Advanced Research Projects Agency of U. S (DARPA); the monochrome image's tracking of man's hiding body-part has been realized by a vision-monitoring system W4 from Maryland university; furthermore, approaches of Hidden Markov Models and Kalman filtering were used for tracking a certain person's position by Gerhard-Mercator university from Germany. On the other hand, the technology of image tracking has also become a major discussion topic in many international periodicals such as PAMI (IEEE Transaction on Pattern Analysis and Machine Intelligence), IJCV (International Journal of

Computer Vision), and several important academic conferences such as CVPR (IEEE Computer Society Conference on Computer Vision and Pattern Recognition), ICCV (International Conference on Computer Vision), etc.

Some achievements in image-tracking have also been gotten at home. Y. R. Du and A. J. Zhou have adopted the approach of optimum matching between the present image-frame's target edge and the real-time updating image-template to determine the target's displacement [1]; in order to solve the blurring complexity in aero-optics, Q. Y. Yang realized the moving target's tracking and de-noising in sequence-images by the approach of image correlation [2]; F. Q. Zhang has studied the underwater complicated environment and analyzed the underwater image's characteristics, then the calculation of inter-frame difference can be conducted on the image sequence, results to the

selecting of an appropriate threshold value for differential image's binarization and segmentation [3]. For balancing the detecting quality and velocity in the process of face recognition, a moving face's detecting and positioning approach in image sequence has been presented by Y. Q. Lei [4]. H. Yuan and Z. P. Lu have used the rotating projection transformation to realize a 3-D meshing coordinate's standardization [5]. D. M. Zhu and G. L. Xu have studied the improving algorithm of moving blur's distinguishing which based on the direction differential [6]. But much deficiency such as instable precision and complicated calculation still exists in their research; therefore more research work must be conducted in this area.

## 2. Algorithm Analysis

### 2.1. Reference Background Studying Based on the Changing Factor

Since a standard background image is difficult to be gotten in the practical environment, and the image is vulnerable to the external interferences which come from the illuminating condition, the moving noise and the external light with time elapsing, thus many pseudo moving-objects will be produced and the accurate tracking of moving vehicle will be obstructed. The Background dynamic updating can debase the background-changing's impact on the moving target's detection, thus it can also be called the background studying, which has the capability of extracting the relative-resting targets and scenery from a image sequence, such as asphalt road surface, separating line, trees and buildings in the traffic monitoring scenery.

For the purpose of extracting and updating the background edge-image, the algorithm can be described as:

$$\begin{aligned} f_{t+1}(x,y) &= [1 - \frac{1}{D_t(x,y)}]f_t(x,y) + \frac{1}{D_t(x,y)}f'_t(x,y) \\ D_t(x,y) &= |f'_t(x,y) - f_t(x,y)|, \end{aligned} \quad (1)$$

where  $f_t(x,y)$  and  $f'_t(x,y)$  are the gray values of a coordinate point  $(x,y)$  in the background edge image and the present image respectively in time  $t$ .  $f_{t+1}(x,y)$  is the background edge image of time  $t+1$ ,  $D_t(x,y)$  is the changing factor, which represents the gray value's difference between the background and the present images at the position of  $(x,y)$ .  $1/D_t(x,y)$  is a learning factor, when  $D_t(x,y)$  is greater, the learning factor becomes smaller, then the new background edge's updating is avianized and the reserving is intensified, and vice versa. When  $D_t(x,y)$  is zero, the road edge is identical to the old background one, thus the edge of old background should be retained. Then the approach of cross

correlation can be applied for the matching of moving-vehicle.

### 2.2. Cross-Correlation Matching

The  $m \times m$  neighborhoods of  $f_t(x,y)$  is selected in which the target is regarded as the center, and a matching template  $a_k(x,y)$  is structured. We use  $a_k(x,y)$  as reference for the acquirement of the identical-size matrix  $b_k(x',y')$  in the image  $f'_t(x,y)$ , and then the value of correlation matching  $\rho(a_k, b_k)$  is reached. When  $\rho(a_k, b_k)$  is greater than or equal to the given threshold  $\delta$ , the coincidental requirement is reached between these two image regions, therefore their center can be labeled as the target's relative position in the image.  $\rho(a_k, b_k)$  is defined as [7]:

$$\rho(a_k, b_k) = \frac{\sum_{a_k, b_k \in S} [a_k(x,y) - \overline{a_k(x,y)}][b_k(x',y') - \overline{b_k(x',y')}]}{\sqrt{\sum_{a_k, b_k \in S} [a_k(x,y) - \overline{a_k(x,y)}]^2} \cdot \sqrt{\sum_{a_k, b_k \in S} [b_k(x',y') - \overline{b_k(x',y')}]^2}} \geq \delta, \quad (1)$$

where  $\overline{a_k(x,y)}$ ,  $\overline{b_k(x',y')}$  are the average values of pixel gray level in  $a_k(x,y)$ ,  $b_k(x',y')$  respectively.

$\sum_{a_k, b_k \in S}$  shows that the calculation is implemented on all the pixels of the window function  $S$  which use the target point as its center.

Determination of the cross correlation threshold  $\delta$ : when the area ratio between the given target and the image is set as  $t$ , the target's gray level distribution is conform to a normal distribution whose probability density function is  $p(z)$ , on the other hand the background is conform to a normal distribution whose probability density function is  $q(z)$ , when the threshold is labeled as  $\delta$ , then  $\int_{-\infty}^{\delta} [t \times p(z) + (1-t) \times q(z)] dz = t$ . Thus  $\delta$  which meets this function is reached as the calculated result.

After the matching and recognizing of the moving vehicle have been finished, the relationship between the target's absolute coordinates  $R(x,y)$  and its relative coordinate  $p_r(x_r, y_r)$  can be listed as follows, then its absolute coordinate can be calculated as [8]:

$$\begin{cases} x = r_{xx}x_l + r_{xy}y_l + r_{xz}z_l + t_{xl} \\ y = r_{yx}x_l + r_{yy}y_l + r_{yz}z_l + t_{yl} \end{cases} \quad (3)$$

$$\begin{cases} x = r_{xx}x_r + r_{xy}y_r + r_{xz}z_r + t_{xr} \\ y = r_{yx}x_r + r_{yy}y_r + r_{yz}z_r + t_{yr} \end{cases}$$

where  $(t_{xl}, t_{yl})$  and  $(t_{xr}, t_{yr})$  are the absolute coordinates of the origin points  $C_l, C_r$  in the coordinate system of  $O(X, Y)$ .

### 2.3. Predicting Operator of Moving Direction

The process of vehicle motion tracking involves not only the vehicle coordinate locating and velocity monitoring, but also the predicting of vehicle moving direction as well. Thus the predicting operator based on area template can be established: as shown in Fig. 1, the central point  $(i, j)$  in the pixel space of image template  $f(x, y)$  is regarded as the core element, the gradient value from each pixel of its neighborhood to the central point  $(i, j)$  can be calculated as:

$$\begin{aligned}
 \nabla_{+x,-y}f(x, y) &= f(x, y) - f(x + 1, y - 1) \\
 \nabla_{-x,+y}f(x, y) &= f(x, y) - f(x - 1, y + 1) \\
 \nabla_{+x,+y}f(x, y) &= f(x, y) - f(x + 1, y + 1) \\
 \nabla_{-x,-y}f(x, y) &= f(x, y) - f(x - 1, y - 1) \\
 \nabla_{-y}f(x, y) &= f(x, y) - f(x, y - 1) \\
 \nabla_{+y}f(x, y) &= f(x, y) - f(x, y + 1) \\
 \nabla_{-x}f(x, y) &= f(x, y) - f(x - 1, y) \\
 \nabla_{+x}f(x, y) &= f(x, y) - f(x + 1, y)
 \end{aligned} \quad (4)$$

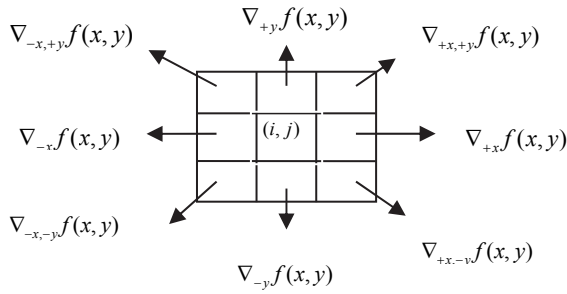


Fig. 1. Predicting operator of area template.

The gradient values in different directions of corresponding points are calculated, and then the gradient values are compared to each other in its peripheral directions. Let  $\omega = |\nabla f(x, y) - \nabla f(x', y')|$ , then the direction characterized by the minimum gradient value is adopted as the optimum direction for direction predicting, after each working cycle is finished the calculation of cross-correlation matching is conducted for determining the direction of predicting operator. By repeatedly calculation and comparison the moving direction of the target vehicle and its motion vector can be easily determined.

### 2.4. Image Mahalanobis Distance

Theory of Mahalanobis distance is shown as follows: mapping image pixels' gray value and their neighborhood's gray value into scattering diagram.

Since object pixel and background ones can be classified into different groups according to their own characters, thus realizing image's region segmentation, Mahalanobis distance segmenting method not only considering Euclidean space distances between individual pixel and group, but also different pixel group's distribution. On the other hand, Mahalanobis distances can label features of image objects and background, assumption of pixel distribution probability is not necessary. Thus Mahalanobis distance can realize image object and background's segmentation sufficiently.

Classical Mahalanobis distance is: [9]

$$\text{Distance}(X, Y) = \sqrt{(X - Y)^{-1} V^{-1} (X - Y)}, \quad (1)$$

where  $X$  is the pending individual's feature,  $Y$  is the certain group's feature,  $V$  is the covariance matrix of different features in this groups. It can be proved that Mahalanobis distance meets three criterion of metric space: positive definite; symmetric and triangle inequality. It can label feature difference between pending individual and group.

Firstly, we build up chromatic three-dimensional space. RGB (primary colour vector) are regarded as three direction dimension of spatial coordinate system, any given pixel can be decomposed into three direction components. Fig. 2 shows this process.



(a) present image (b) background image

Fig. 2. Image background without changing factor.

Next, by use of Mahalanobis distance in chromatic image's segmentation, divides image into several regions roughly according to colour distribution. Colours in one region are identify or closing.

$$\begin{aligned}
 F &= \{F_1(x, y), F_2(x, y), \dots, F_N(x, y)\} \\
 &= \{(F_1(x, y) + F_2(x, y) + \dots + F_N(x, y) = F(x, y))\} \quad (6)
 \end{aligned}$$

where  $F_1(x, y), F_2(x, y), \dots, F_N(x, y)$  is the several roughly divided colour region.

Selecting segmenting object pixel  $f(x, y)$  and pending pixel  $g(x', y')$  in one image colour region  $F_i(x, y), 1 \leq i \leq N$ . We label their  $3 \times 3$

neighborhoods as  $S_f(x,y)$  and  $S_g(x',y')$  respectively. Then decompose these two pixels into three colour vectors:

$$f(x,y) = \{f_r(x,y), f_b(x,y), f_g(x,y)\}$$

$$g(x',y') = \{g_r(x',y'), g_b(x',y'), g_g(x',y')\}.$$

Thus Mahalanobis distance between this segmenting pixel pair  $(f(x,y),g(x',y'))$  is defined as:

$$\left\{ \begin{array}{l} Maha\_Dist(r) = \sqrt{((f_r - \mu_{f,r})(g_r - \mu_{g,r}))V_r^{-1}((f_r - \mu_{f,r})(g_r - \mu_{g,r}))^{-1}}, \\ Maha\_Dist(b) = \sqrt{((f_b - \mu_{f,b})(g_b - \mu_{g,b}))V_b^{-1}((f_b - \mu_{f,b})(g_b - \mu_{g,b}))^{-1}} \\ Maha\_Dist(g) = \sqrt{((f_g - \mu_{f,g})(g_g - \mu_{g,g}))V_g^{-1}((f_g - \mu_{f,g})(g_g - \mu_{g,g}))^{-1}} \end{array} \right. \quad (7)$$

where  $u_{f,r}, u_{f,b}, u_{f,g}$  are the neighborhood  $S_f(x,y)$  three vectors' mean values;  $u_{g,r}, u_{g,b}, u_{g,g}$  are the neighborhood  $S_g(x',y')$  three vectors' mean values; matrix  $V_i$  is the covariance matrix between two  $3 \times 3$  neighborhoods  $S_f(x,y)$  and  $S_g(x',y')$ .

$$V_r = \begin{pmatrix} \sigma_{fr}^2 & r\sigma_{fr}\sigma_{gr} \\ r\sigma_{fr}\sigma_{gr} & \sigma_{gr}^2 \end{pmatrix}, \quad (8)$$

$$V_r^{-1} = \frac{1}{\sigma_{fr}^2\sigma_{gr}^2(1-r^2)} \begin{pmatrix} \sigma_{gr}^2 & -r\sigma_{fr}\sigma_{gr} \\ -r\sigma_{fr}\sigma_{gr} & \sigma_{fr}^2 \end{pmatrix}$$

where  $\sigma_{fr}$  and  $\sigma_{gr}$  are the  $S_f(x,y)$  and  $S_g(x',y')$  's standard deviation,  $r$  is the correlation coefficient between  $S_f(x,y)$  and  $S_g(x',y')$ . If correlation is significant, probability of these two neighborhoods that belong to identified or close region is greater, otherwise probability is smaller. Through transformation, Mahalanobis distance practical calculating equation is gotten, it is shown by Eq. 9:

$$\left\{ \begin{array}{l} Distance(r)^2 = \frac{(f_r - \mu_{f,r})^2}{\sigma_{f,r}^2(1-r^2)} + \frac{(g_r - \mu_{g,r})^2}{\sigma_{g,r}^2(1-r^2)} - \frac{2r(f_r - \mu_{f,r})(g_r - \mu_{g,r})}{\sigma_{f,r}\sigma_{g,r}(1-r^2)} \\ Distance(b)^2 = \frac{(f_b - \mu_{f,b})^2}{\sigma_{f,b}^2(1-r^2)} + \frac{(g_b - \mu_{g,b})^2}{\sigma_{g,b}^2(1-r^2)} - \frac{2r(f_b - \mu_{f,b})(g_b - \mu_{g,b})}{\sigma_{f,b}\sigma_{g,b}(1-r^2)} \\ Distance(g)^2 = \frac{(f_g - \mu_{f,g})^2}{\sigma_{f,g}^2(1-r^2)} + \frac{(g_g - \mu_{g,g})^2}{\sigma_{g,g}^2(1-r^2)} - \frac{2r(f_g - \mu_{f,g})(g_g - \mu_{g,g})}{\sigma_{f,g}\sigma_{g,g}(1-r^2)} \end{array} \right. \quad (9)$$

**Definition:**  $z$  is a given pixel in RGB chromatic space  $a$  is colour center of image region, if space distance between  $z$  and  $a$  is less than preset threshold  $D_0$ , thus  $z$  and  $a$  are regarded as pixels in similar or identical region. Basic Euclidean space distance  $D_0$  is defined as:[10]

$$D(z,a) = \|z - a\| = [(z - a)^T(z - a)]^{\frac{1}{2}} = [(z_R - a_R)^2 + (z_G - a_G)^2 + (z_B - a_B)^2]^{\frac{1}{2}}$$

According to Euclidean space distance, improved chromatic image's segmenting Mahalanobis distance can be defined as:

$$mahalanobis\_dist = \frac{1}{\sqrt{(Distance(r))^2 + Distance(b)^2 + Distance(g)^2}}, \quad (10)$$

where  $Distance(r)$ ,  $Distance(b)$ ,  $Distance(g)$  are the Mahalanobis distances of three chromatic components between two image pixels.

Through calculating Mahalanobis distance between object pixel and each armed ones by sequence, Mahalanobis distance histogram is generated. X axis represents Mahalanobis space distance between these two pixels, Y axis is appearance probability of different Mahalanobis space distance. According to Mahalanobis distance between different pairs of colour region's pixels, chromatic image's pixels are classified into different distance clustering [11].

In each pixel clustering interval, variance between clusters is calculated. Centre pixel is regarded as space segmentation center, using Mahalanobis distance between object pixel and center pixel as processing parameter. Segmenting threshold value can be defined as average value of this region's Mahalanobis distance of each pair of pixels. If actual distance is greater than segmenting threshold value, object pixel is regarded as outer region pixel (including the background pixel), otherwise it is regarded as inner region ones. Thus optimum segmenting thresholds of each interval are gotten.

A chromatic image includes several different colour regions, so several crests and hollows are shown in space distance histogram. Histogram can be divided into different threshold intervals. Assuming Mahalanobis distance histogram is divided into  $n$  threshold intervals, each interval is divided into two groups:  $C_{i0}$  and  $C_{i1}$ . Final variance between clusters is:

$$\sigma^2 = \sum_{i=1}^n \max \sigma_i^2 = \sum_{i=1}^n \max w_{i0} w_{i1} (u_{i0} - u_{i1})^2, \quad (11)$$

where  $u_i$  is the mean of each segmenting threshold interval,  $\sigma_i^2$  is the variance of each segmenting threshold interval,  $w_{ij} (i=1,2,\dots,n, j=0,1)$  is the each class's appearance probability, Mahalanobis space distance  $\delta$  that makes variance maximum is selected as optimum image-segmenting threshold:

$$\delta^* = \arg \max \sigma_k^2.$$

After thresholds of each Mahalanobis distance interval are determined, segmentation is implemented. Object pixel's chromatic parameters are used as reference; Mahalanobis distances between pair of object pixel and each armed ones are compared with given threshold. Then each armed pixel is classified into specific chromatic region and vested a certain preset false colour to identify

different region that it belongs to. Specific procedure is shown in Eq. 12 [12, 13].

$$\left\{ \begin{array}{l} \text{if } \text{threshold}_1 < \text{distance} < \text{threshold}_2, \\ \quad f(i, j) = [R_1, G_1, B_1] \\ \text{if } \text{threshold}_2 < \text{distance} < \text{threshold}_3, \\ \quad f(i, j) = [R_2, G_2, B_2] \\ \quad \vdots \\ \text{if } \text{threshold}_{n-1} < \text{distance} < \text{threshold}_n, \\ \quad f(i, j) = [R_{n-1}, G_{n-1}, B_{n-1}] \end{array} \right. \quad (12)$$

where  $\text{threshold}_n$  is the No.  $i$  image Mahalanobis distance segmenting threshold, distance is Mahalanobis distance between object pixel and armed pixel.  $f(i, j) = [R_{n-1}, G_{n-1}, B_{n-1}]$  is treated pixel's false colour.

### 3. Tracking Experiment

The image sequence about the moving vehicles is acquired in the expressway of Guangzhou urban area, which covers a practical area of  $20\text{ m} \times 20\text{ m}$ , as can be seen in Fig. 2. The digital image acquiring system of SONY HDR-XR150E from Yue-Jing high tech Co. is chosen for the  $2000 \times 2000$  pixel points' coordinate-acquainting along  $u, v$  directions respectively. Matlab7.0 is used for programming the kernel analysis module. Other experiment conditions are: Celeron 2.26 microprocessor, 256 M memory, operation system is Windows XP.

First the image sequence of moving vehicles in the time duration of 80 s is acquired, which has the speed of image sampling at 24 frame/s. the operator of canny is selected for the segmentation between the foreground target and the background environment. With Eq. (1) the extracting and updating of the background edge image based on the changing factor is conducted, thus the sequence of background image without external interference can be obtained. The background edge-image without the changing factor is shown in Fig. 2, it can be seen that the contour track of the passing bus still exists in the certain image region, as many noise points still retained in the image background, which adversely affects the accuracy and reliability of following image detection; on the other hands, the image sequence with the changing factor is shown in Fig. 3, from this figure it can be reached that the contour shadow from the passing bus is debated markedly, thus the noise points can be eliminated and the following updating of background image can be conducted more stably.

The key Matlab program is programmed as:

```
f2 = abs( f - cdB );
f2 = uint8(f2);
bwf = f2;
f3=double(f2);
sum=0;
for a = 1:s(1)
```

```
for b = 1:s(2)
sum=sum+f3(a,b);
end
end
sum=sum/s(1)/s(2);
bw = find( f2 < 38 );
bwf(bw) = 0;
sum=(sum+2)*2.5;
if sum ==0
cdB(bw) =cdB(bw) ;
else
cdB(bw) = f(bw)/sum+(cdB(bw))*(1-1/sum);
end
bw = find( f2 >= 38 );
bwf(bw) = 255;
cdB = uint8(cdB);
f2 = abs( f - cdB );
bw = find( f2 < 38 ); bwf(bw) = 0;
bw = find( f2 >= 38 ); bwf(bw) = 255;
```



(a) present frame image (b) background image

Fig. 3. Image background with changing factor.

Two detecting lines are defined in the imaging region, which facilitates the counting and speed-information's extracting of the target vehicles. The detecting window is determined by the practical environment, following requirements should be reached simultaneously: the lines are perpendicular to the vehicle driving direction; all lines are parallel to each other; the minimum spacing between these two lines is greater than the maximum length of vehicle, etc. The black lines are used for the driving detection, and the spacing between them is the detecting region, as illustrated in Fig. 4. All the passing vehicles are tracked automatically by the red frames, which are showed by Fig. 5.



Fig. 4. Detecting region.

Fig. 5. Tracking frame.

The calculating equation of the vehicle driving speed is [14, 15]:

$$V = \frac{S}{(N_2 - N_1) \times (1/F_r)}, \quad (13)$$

where V is the vehicle speed, S is the spacing between these two detecting lines; N1 and N2 are the numbers of the image frame when the target vehicle reaches these two detecting lines respectively; the length of S is 21 m according to National Road

Indicative Mark (NRIM), as illustrated in Fig. 6 [16]. Other parameters are obtained by the program command.

Through calculating the segmenting results of moving vehicle can be obtained as showed in Fig 7: the image of moving vehicle at the present frame is shown at the left; the reference background with the changing factor is shown at the middle; and the target vehicle after a process of completely segmentation is shown at the right, and several key tracking parameters are listed in Table 1.



Fig. 6 National road indicative mark



Fig. 7 Segmentation of moving vehicle:  
Left: present frame image Middle: background image Right: segmenting result of moving vehicle.

Table 1. Key tracking parameter.

No of vehicle	Coordinate entering region	Coordinate leaving region	Speed (km/h)	Detecting duration
1	(87,86)	(139,239)	57	4.15S
2	(117,86)	(144, 239)	61	4.47S
3	(106, 86)	(102, 239)	44	5.84S
4	(124, 86)	(85, 239)	55	4.06S
5	(75, 86)	(94, 239)	49	3.17S
6	(94, 86)	(88, 239)	63	2.08S
7	(79, 86)	(106, 239)	71	1.46S
8	(118, 86)	(99, 239)	54	3.59S

The key Matlab program is:  
 info=aviinfo(str);  
 FPS=info.FramesPerSecond;  
 if mid<155  
 if (zlt==0 && bottom > 42 && bottom < 52 && c1-eflt>12)  
 eflt=c1;  
 else zlt=1;  
 end

```

    if (zlt==1 && bottom > 156 && bottom < 182 && area > 1000 && c1-eflt > 12 )
        eelt=c1;
    else zlt=0;
    speedlt=round((21/((eelt-eflt)*1/FPS))*3.6);
    ssl=strcat(num2str(speedlt),'Km/h');
    set(handles.text1,'string',ssl);
    cll=c1+1;
    set(handles.text3,'string',num2str(c1));
    
```

```

csl=strcat(pn,num2str(cll),num2str(speedt));
    imwrite(colourFrC,csl)
    end
    end
    if mid>146
        if (zrt==0&&bottom > 42&&bottom <
52&&c1-efrt>12)
            efrt=c1;
        else zrt=1;
        end
        if (zrt==1&&bottom >156&&bottom <200&&c1-
eert>25 )
            eert=c1;
            zrt=0;          speedrt=round((21/((eert-
efrt)*1/FPS))*3.6);
            ssr=strcat(num2str(speedrt),'Km/h');
            set(handles.text2,'string',ssr);
            cll=cll+1;
        set(handles.text3,'string',num2str(cll));
        csr=strcat(pn,num2str(cll),num2str(speedrt));
        imwrite(colourFrC,csr)
        end
    end
end

```

According to Eq. (4) the neighborhood direction operators of the target vehicle motion coordination are established, then the prediction of the vehicle coordinate location and moving velocity in the next frame can be realized. Through the contrasting between the predicting result and the practical condition, the accuracy of image tracking can be amended and guaranteed. The predicting results of

moving vehicles' coordinate location and their motion vector at several key points are listed in Table 2. It can be reached that the accurate results of vehicle moving direction and speed can be obtained by the direction predicting operator, thus the accuracy and validity of image tracking can also be ensured [16, 17].

Finally for the purpose of evaluating this new algorithm, this new algorithm is compared with other frequently-used image tracking approach in the process of moving-vehicle tracking, such as the approach of background subtracting, approach of morphological processing, approach of Hausdorff distance detecting, approach of centroid iterating and approach of particle filtering [18-20]. The comparing conditions are listed as follows: the speed range of target vehicle is 20 km/h~35 km/h; the time duration of image tracking is 50 s, the size of sequence image is 2800×1280. The process of comparison is implemented in many aspects, such as the precision of target's coordinate location, error of target's speed, time-consuming of calculating process, complex rates of each algorithm, noise ratio of target vehicle, time delay of image tracking, etc. The comparing results are listed in Table 3 and the conclusions can be reached that, in the condition of homogeneous precision and recognition rate, this new algorithm can markedly simplifies the calculating process and develops the processing speed, therefore it can be proved that this new algorithm is appropriate for the moving target's tracking in the area of traffic flow's monitoring.

**Table 2.** The predicted point and velocity vector of some key points.

No.	Predicted coordinate	Practical coordinate	Velocity vector	Velocity
1	(422,436)	(422,436)	(28,14)	33.54km/h
2	(434,1270)	(434,1270)	(41,13)	34.18km/s
3	(308,2110)	(308,2110)	(160,13)	35.14 km/h
4	(416,1948)	(416,1948)	(17,8)	37.13 km/h
5	(1706,2488)	(1706,2488)	(79,11)	33.35 km/h
6	(1640,2182)	(1640,2182)	(15,13)	40.12 km/h
7	(2212,1732)	(2212,1732)	(14,13)	42.14 km/h
8	(2372,1150)	(2372,1150)	(15,17)	35.76 km/h
9	(2378,430)	(2378,430)	(28,13)	42.67 km/h
10	(1358,460)	(1358,460)	(22,13)	37.56 km/h

**Table 3.** Performance comparison of different tracking approaches.

Algorithm	Coordinate accuracy (accurate coordinate/ total coordinate×100 %)	Average speed precision (speed error/ speed×100 %)	Noise ratio of target vehicle (error/ total number×100 %)	Complex rate of algorithm	Time delay of tracking(s)	Average time-consuming in calculation(s)
New algorithm	95.23 %	3.152 %	2.46 %	$n^3+3n^2+4$	0.2 s	3.87 S
Background subtracting	86.49 %	4.891 %	3.34 %	$4n^4+5n^3+2n^2$	1.12 s	4.95 S
Morphological processing	88.71 %	3.718 %	5.72 %	$2n^3+3n^2+4n$	1.03 s	5.77 S
Hausdorff distance	73.96 %	2.489 %	7.78 %	$3n^3+3n^2+7n$	0.85 s	5.17 S
Centroid iterating	79.16 %	1.877 %	8.89 %	$3n^3+2n^2+4n^2$	0.62 s	4.88 S
Particle filtering	85.38 %	3.095 %	4.43 %	$6n^3+3n^2+4n$	0.44 s	6.19 S

## 4. Conclusions

By using the moving vehicle as an example, a new image tracking approach on static background is investigated and the software system is developed. Through the changing factor is set, the reference background's learning is conducted, and then the cross-correlation matching and coordinate transformation are adopted for tracking the target vehicle, the vehicle speed is measured by setting the detecting lines in the image sequence. Combining with the direction predicting operator, the target vehicle traveling direction and traveling velocity can be predicted. On Matlab software platform the kernel module and GUI interface are designed and debugged. It proves that this algorithm can adapt to the variation of external environment and decrease the interruption of scenery camera, thus a rapid and accurate tracking result of moving vehicle can be achieved.

## Acknowledgements

The author acknowledges the funding of following science foundation: National Natural Science Foundation of China (No. 51205073), China Postdoctoral Science Foundation funded project (No. 2013T60797, No. 2012M510197), China National Spark Program (No. 2013GA780063); the science and technology project of Guangzhou city (No. 2012J4100053, 12C42011566), Foundation Project of The State Key Laboratory of Fluid Power Transmission and Control, Zhejiang University (No. GZKF-201201), Foundation Project of Traction Power State Key Laboratory, Southwest Jiaotong University (No. TPL1311) and Foundation Project of the National Engineering Research Centre of Near-Net-Shape Forming for Metallic Materials, South China University of Technology (No. 2012007) are also appreciated for supporting this work.

## References

- [1]. Y. R. Du, A. J. Zhou. A tracking approach of mobile vehicle based on video sequence images, *Journal of Electronic Measurement and Instrument*, Vol. 23, Issue 3, 2009, pp. 45-48.
- [2]. Q. Y. Yang. Tracking and simulation for motion of relativity small target images, *Journal of System Simulation*, Vol. 20, Issue 6, 2008, pp. 1645-1653.
- [3]. F. Q. Zhang, C. D. Zheng. Real time detecting algorithm for underwater moving targets, *Acta Photonica Sinica*, 2009, Vol. 38, Issue 6, 2009, pp. 1557-1560.
- [4]. Y. Q. Lei, X. X. Liu. Face detection and feature location of moving men in video, *Journal of South China University of Technology*, Vol. 37, Issue 5, 2009, pp. 31-37.
- [5]. H. Yuan, Z. P. Yu. Pose normalization of 32D mesh model based on rotation transformation, *Journal of Agriculture Engineering*, Vol. 22, Issue 6, 2009, pp. 61-67.
- [6]. D. M. Zhu, G. L. Xu. Improved approach of directional derivation to identify the direction of motion blurred image, *Aero Weaponry*, Vol. 3, Issue 7, 2009, pp. 43-46.
- [7]. L. Zheng. Application of ANN in recognition of target image, *Journal of Beijing Institute of Technology*, Vol. 17, Issue 8, 1997, pp. 493-498.
- [8]. Shi Min, A prediction based vector quantization approach for image coding, *Journal of South China University of Technology*, Vol. 34, Issue 1, 2006, pp. 18-23.
- [9]. Gwang Hoon Rhee, Hyung Jin Sung. Numerical prediction of locally forced turbulent separated and reattaching flow, *Fluid Dynamics Research*, Vol. 26, Issue 6, 2000, pp. 421-436.
- [10]. Song Chun-Lin, Feng Rui, Liu Fu-Qiang. A novel fractal wavelet image compression approach, *Journal of China University of Mining & Technology: English Edition*, Vol. 17, Issue 3, 2007, pp. 121-125.
- [11]. Wang Lijuan, Rui Yannian, Jiang Xiaomei. The quality evaluation approaches for chip package based on the theory fuzzy grey, *Machine Design and Research*, Vol. 24, Issue 6, 2008, pp. 91-94.
- [12]. Kun Li-Wen. Weighted grey relation grade, *The Journal of Grey Systems*, Vol. 23, Issue 4, 2005, pp. 27-29.
- [13]. E. A. Luke, P. Cinnella, Numerical simulations of mixtures of fluids using upwind algorithms, *Computers & Fluids*, Vol. 36, Issue 10, 2007, pp. 1547-1566.
- [14]. Ding-An Chiang, Louis R. Chow, Nan-Chen Hsien, Fuzzy information in extended fuzzy relational databases, *Fuzzy Sets and Systems*, Vol. 92, Issue 10, 1997, pp. 1-20.
- [15]. Xiaohui Tang, Guoqing Chen, Equivalence and transformation of extended algebraic operators in fuzzy relational databases, *Fuzzy Sets and Systems*, Vol. 157, Issue 20, 2006, pp. 1581-1596.
- [16]. C. M. B. Nobre, R. A. Braga Jr, A. G. Costa, R. R. Cardoso, W. S. da Silva, T. Sáfadi, Bio-speckle. Laser spectral analysis under inertia moment, entropy and cross-spectrum methods, *Optics Communications*, Vol. 282, Issue 1, 2009, pp. 2236-2242.
- [17]. Deniz Erdogmus, Erik G. Larsson, Rui Yan, Jose C. Principe, Jeffrey R. Fitzsimmons, Measuring the signal-to-noise ratio in magnetic resonance imaging: a caveat, *Signal Processing*, Vol. 84, Issue 10, 2004, pp. 1035-1040.
- [18]. Jingyu Hua, Limin Meng, Zhijiang Xu, Gang Li, An adaptive signal-to-noise ratio estimator in mobile communication channels, *Digital Signal Processing*, Vol. 20, Issue 12, 2010, pp. 692-698.
- [19]. Y. Z. Chen, Complex potentials and singular integral equation for curve crack problem in antiplane elasticity, *International Journal of Engineering Science*, Vol. 38, Issue 3, 2000, pp. 565-574.
- [20]. Michael Griebel, Gerhard Zumbusch, Parallel adaptive subspace correction schemes with applications to elasticity, *Computer Methods in Applied Mechanics and Engineering*, Vol. 184, Issue 10, 2000, pp. 303-332.